ADVANCED ELECTRONIC MATERIALS

Supporting Information

for *Adv. Electron. Mater.*, DOI: 10.1002/aelm.202000195

High-Performance Zinc Tin Oxide TFTs with Active Layers Deposited by Atomic Layer Deposition

Christopher R. Allemang, Tae H. Cho, Orlando Trejo, Shantam Ravan, Robin E. Rodríguez, Neil P. Dasgupta, and Rebecca L. Peterson**

Supporting Information

High-Performance Zinc-Tin-Oxide TFTs with Active Layers Deposited by Atomic Layer Deposition

Christopher R. Allemang, Tae H. Cho, Orlando Trejo, Shantam Ravan, Robin E. Rodríguez, Neil P. Dasgupta, Rebecca L. Peterson**

C. R. Allemang, S. Ravan, Prof. R. L. Peterson
Electrical Engineering and Computer Science Department, University of Michigan, Ann Arbor, MI 48109, USA
E-mail: blpeters@umich.edu

T. H. Cho, Dr. O. Trejo, R. E. Rodríguez, Prof. N. P. Dasgupta
Department of Mechanical Engineering, University of Michigan, Ann Arbor, MI 48109, USA
E-mail: ndasgupt@umich.edu

Table S1 Film thickness measured by ellipsometry. Measurements were taken on as-deposited films unless otherwise stated.

f_{Sn}	c_{Sn}	ALD Deposition Temperature	ALD Deposition Type	Thickness [nm]	Related Figures and Tables
0	0	150 ºC	Thermal	22	Fig. 3b, 3c, S2
25%	14%	150 ºC	Thermal	25	Fig. 2a, 3c, S2
33%	18%	150 ºC	Thermal	25	Fig. 2a, 3c, S2
45%	21%	150 ºC	Thermal	22	Fig. 2a, 2c, 3b, 3c, 4a, 4c, 7a, 7c, S2, S3a, S3c, S6 Table 1, S2, S4, S5
45%	21%	200 ºC	Thermal	5.0	Fig. 7b, 7d Table S6
45%	21%	200 ºC	Thermal	9.9 8.9[a)]	Fig. 5a, 5c, 7b, 7d Table 1, S2, S6
45%	21%	200 ºC	Thermal	13	Fig. 2b, 6a, 6b, 7b, 7d, S1a Table S3, S4, S6
45%		150 ºC	Hybrid	19	Fig. 4b, 4c, S3b, S3d Table 1, S2
45%	21%	200 ºC	Hybrid	22	Fig. 5b, 5d, 6a, Table 1, S2
50%	26%	150 ºC	Thermal	12	Fig. 1b, 3b, 3c, S2
55%	32%	150 ºC	Thermal	26	Fig. 1b, 3c, S2
66%	37%	150 ºC	Thermal	11	Fig. 1b, 3b, 3c, S2

[a)] 500°C annealed

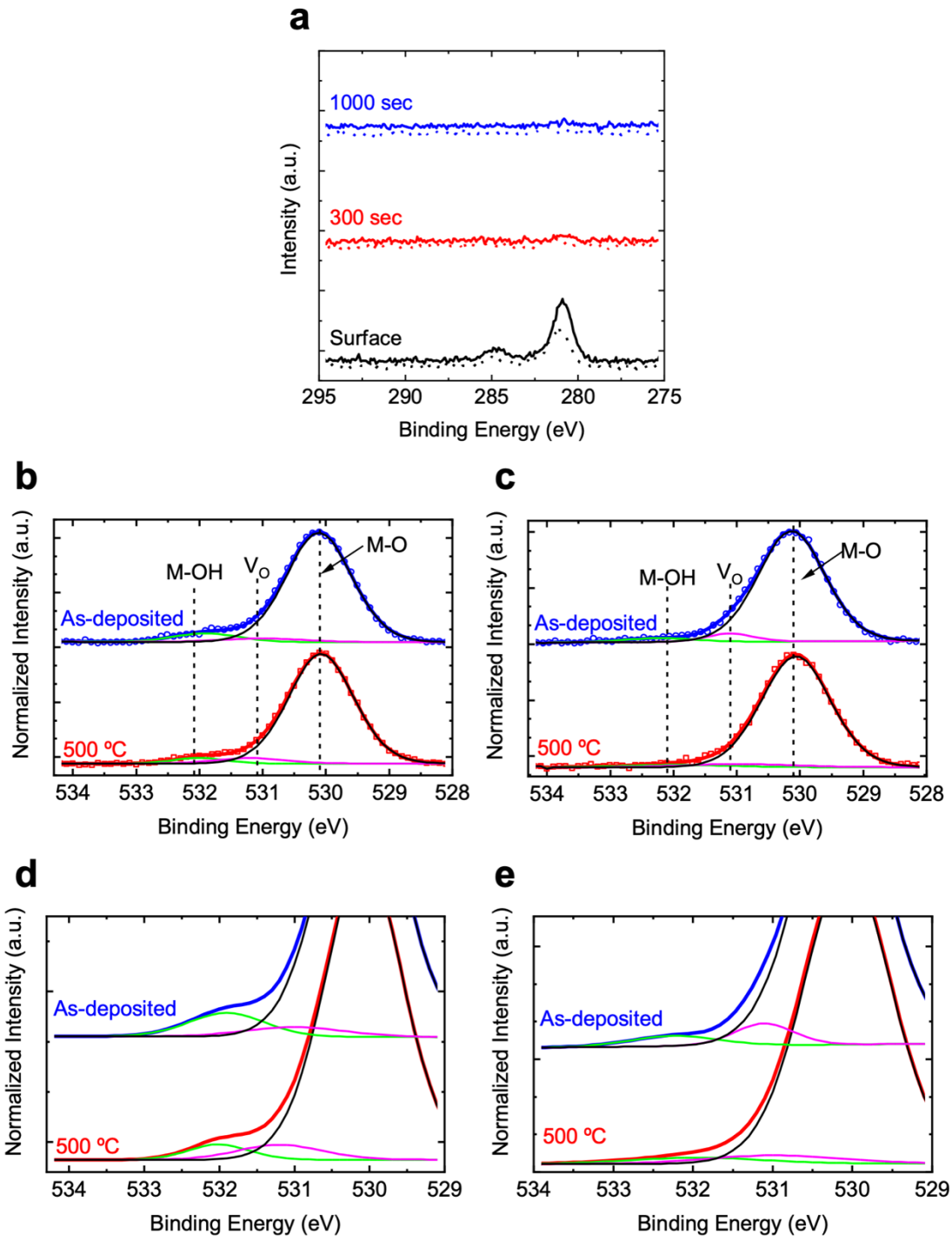

Figure S1. a) Carbon XPS core scans of 21% tin composition films deposited at 200 ºC using thermal ALD. Scans were taken at the surface and after Ar sputtering of various durations to measure bulk film properties. Both as-deposited (solid lines) and annealed films at 500 ºC (dotted lines) show carbon at the film surface. After 300 sec of sputtering, the amount of carbon is below

the detection limit of XPS, ~ 0.1 at %. b,c) O 1s XPS spectra acquired after Ar sputtering of ZTO ALD films as-deposited (blue circles) and after 500 ºC anneal (red squares). The solid lines indicate fits using the atomic percentages of metal-oxygen bonds (black), M-O, oxygen vacancies (pink), V_O, and metal-hydroxide bonds (green), M-OH, listed in Table S3. Spectra for two ZTO films are shown: b) thermal ALD at 150 ºC; c) hybrid ALD at 200 ºC. The O 1s XPS spectra for thermal ALD at 200 ºC are shown in Figure 6b. d) and e), zoomed in spectra showing only the Gaussian fits of b) and c), respectively. The XPS curves shown in b,c,d, and e) were normalized to the M-O peak height of each film.

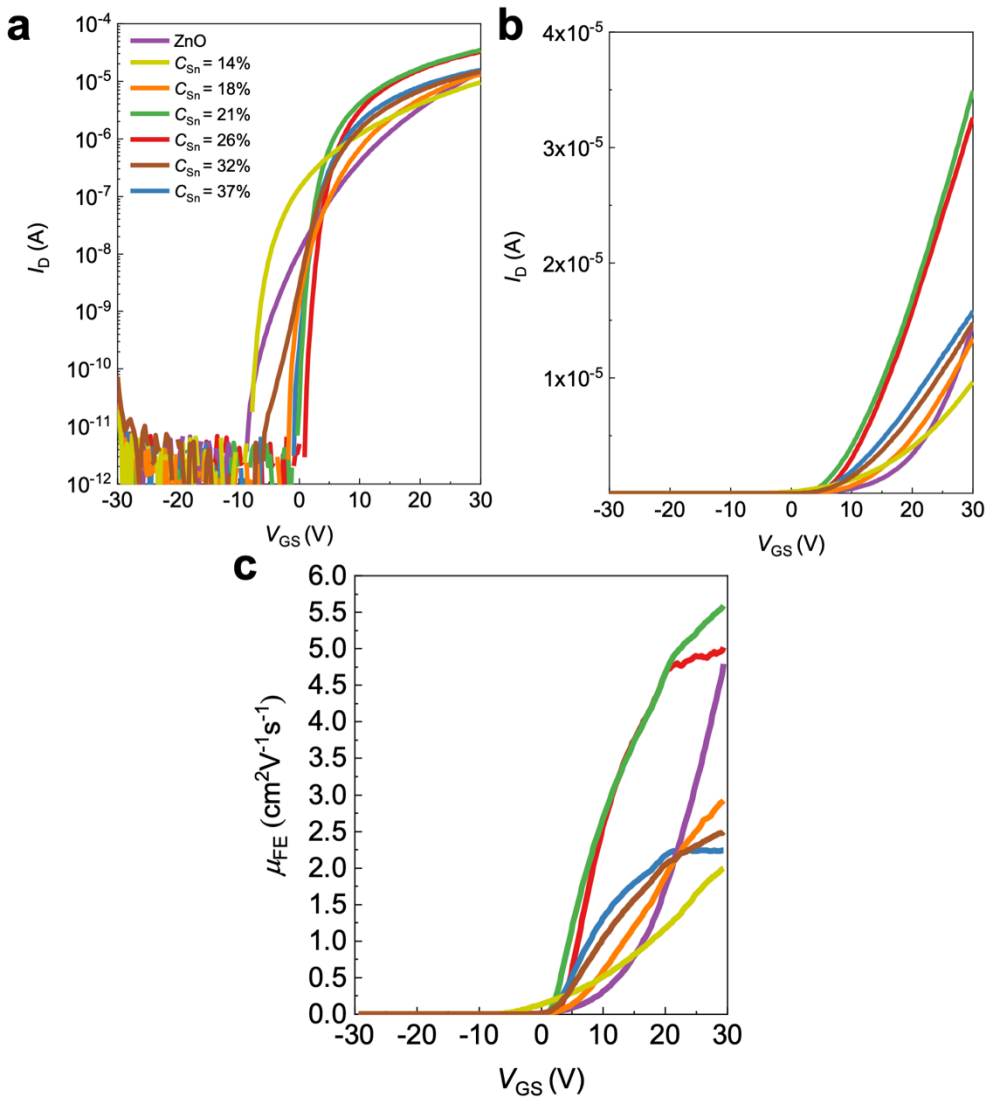

Figure S2. Transfer curves of ZTO for various tin compositions, measured by XPS. All ZTO films were deposited using the thermal process at 150 ºC and annealed at 500 ºC with W/L of 10 and V_{DS} = 1 V plotted on a) semi-logarithmic scale and b) linear scale. c) Mobility vs. V_{GS} plot extracted from transfer curves. The c_{Sn} = 0%, 21%, 26%, and 37% curves in Figure S2a are identical to those shown in Figure 3b.

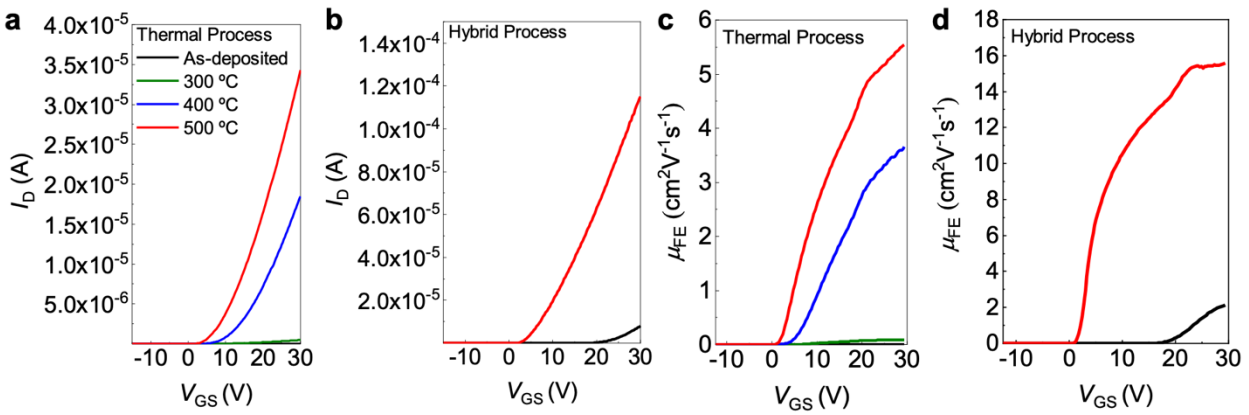

Figure S3. a,b) Linear *I-V* transfer curves and c,d) field-effect mobility for the *I-V* curves shown in Figure 4a and Figure 4b. All ZTO TFTs have f_{Sn} = 45% films deposited at 150 ºC. a,c) ZTO deposited by thermal ALD; b,d) ZTO deposited using the hybrid ALD process. All TFTs have W/L of 10 and V_{DS} = 1 V.

Table S2. Comparison of previously published ALD ZTO TFTs with those reported in this work.

The results shown here have the highest mobility reported to date for ALD ZTO TFTs.

ALD Deposition Temperature	ALD Oxidant	Anneal Temperature	Tin composition	μ_{FE} [$cm^2V^{-1}s^{-1}$]	*SS* [V dec^{-1}]	Ref.
200 ºC	**Hybrid**	**None**	**21%**	**13.8** [d]	**0.43**	**This Work**
170 ºC	Thermal (H_2O_2)	250 ºC	20%	9-10 [a]	0.97	[1]
200 ºC	**Hybrid**	**300 ºC**	**21%**	**18.8** [d]	**0.31**	**This Work**
170 ºC	Thermal (H_2O_2)	350 ºC	20%	11-12 [a]	0.27	[1]
150 ºC	Thermal (H_2O_2)	400 ºC	50% [b]	13.2 [c]	0.15	[2]
200 ºC	**Thermal (H_2O)**	**400 ºC**	**21%**	**16.1** [d]	**0.37**	**This Work**
200 ºC	**Hybrid**	**400 ºC**	**21%**	**22.1** [d]	**0.29**	**This Work**
170 ºC	Thermal (H_2O_2)	450 ºC	20%	12-13 [a]	0.27	[1]
170 ºC	Thermal (H_2O_2)	450 ºC	18%	12-13 [a]	?	[1]
170 ºC	Thermal (H_2O_2)	450 ºC	23%	12-13 [a]	?	[1]
170 ºC	Thermal (H_2O_2)	450 ºC	31%	10 [a]	?	[1]
170 ºC	Thermal (H_2O_2)	450 ºC	53%	5 [a]	?	[1]
120 ºC	Thermal (H_2O_2)	450 ºC	18%	3.4 [a]	?	[1]
120 ºC	Thermal (H_2O_2)	450 ºC	23%	2.5 [a]	?	[1]
120 ºC	Thermal (H_2O_2)	450 ºC	31%	1.5 [a]	?	[1]
120 ºC	Thermal (H_2O_2)	450 ºC	53%	1.75 [a]	?	[1]
150 ºC	**Hybrid**	**500 ºC**	**45%** [b]	**15.5** [d]	**0.29**	**This Work**
150 ºC	Thermal (H_2O_2)	500 ºC	50% [b]	4.8 [c]	0.27	[2]
200ºC	**Thermal (H_2O)**	**500 ºC**	**21%**	**17.5** [d]	**0.30**	**This Work**
200ºC	**O_2 Plasma**	**500 ºC**	**45%** [b]	**22.7** [d]	**0.36**	**This Work**
200 ºC	**Hybrid**	**500 ºC**	**21%**	**22.0** [d]	**0.28**	**This Work**

a) Mobility extracted for V_{DS} = 0.1 V.
b) Tin cycle fraction reported because composition fraction was not available.
c) Mobility extracted for V_{DS} = 10 V.
d) Mobility extracted for V_{DS} = 1 V.

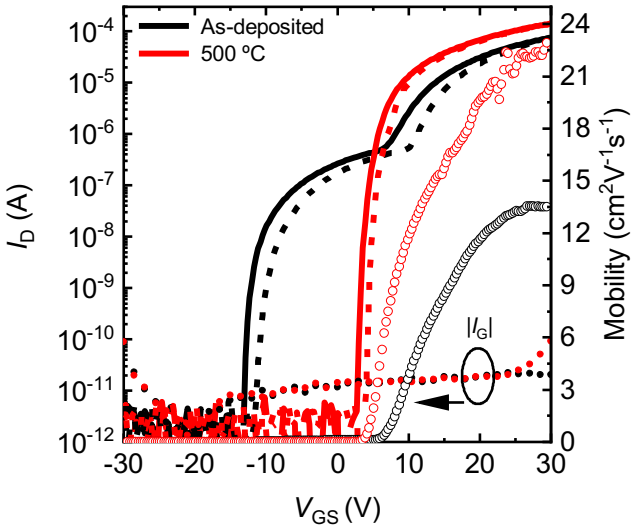

Figure S4. Transfer curves of f_{Sn} = 45% films deposited at 200 ºC using an all-plasma process, as-deposited and after a 500 ºC anneal. The forward *I-V* curves are indicated by the solid lines, the reverse curves are indicated by the dashed lines, and the $|I_G|$ is indicated using solid dots, all plotted on the left y-axis. Mobility is plotted using the open circles on the right y-axis. For both devices, W/L = 10, and V_{DS} = 1 V. The as-deposited films show a kink in the subthreshold I_D indicative of a large number of defects. Annealing these films at 500 ºC removes some of these defects yielding rapid turn-on.

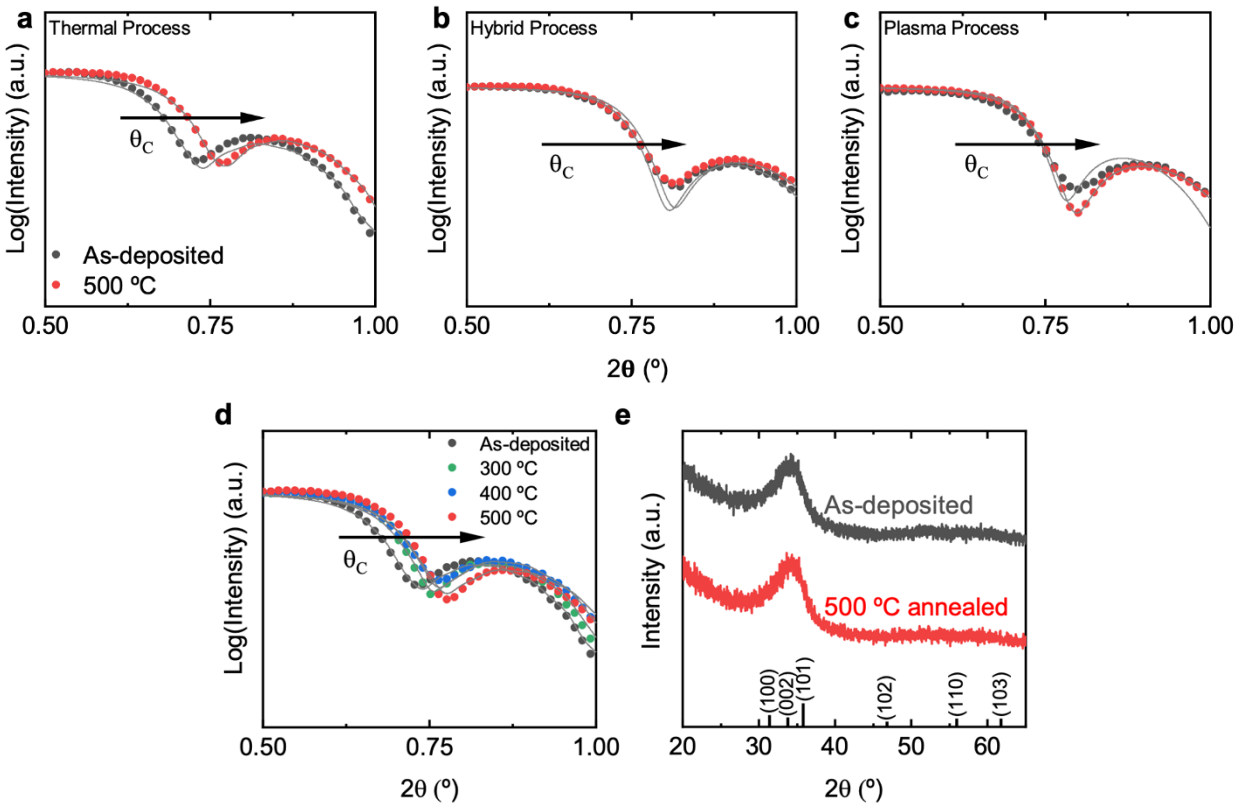

Figure S5. Normalized XRR of f_{Sn} = 45% ZTO films deposited: a,b,c) at 200 ºC using the a) thermal, b) hybrid, or c) all-plasma ALD process. XRR spectra are shown for as-deposited films and film annealed at 500 ºC; d) at 150 ºC using the thermal ALD process, comparing as-deposited film to those annealed at various temperatures. In all plots, open circles are measured data and lines are simulated fits. The critical angle shifts further right as anneal temperature increases, indicating an increase in density. The fit values of ZTO density can be found in Table S4. These films correspond to the TFT devices shown in Figure 4, Figure 5, and Figure S4. The increase in electron mobility after annealing is correlated with an increase in ZTO film density. e) XRD for a ZTO film deposited by hybrid ALD at 200 ºC with f_{Sn} = 45%, showing that both films are amorphous and the film phase does not change upon post-deposition anneal. ZnO peak positions (JCPDS No. 36-1451) are shown at the bottom.

Table S3. Atomic fractions of oxygen atom components for various ALD ZTO films. The table indicates oxygen found in three environments: (1) fully oxidized surroundings (M-O); (2) in oxygen-deficient regions (V_O); and (3) in hydroxyls (M-OH). The fractions are obtained by deconvolution of the O 1s XPS spectra shown in Figure 6b and Figure S1b,c,d,e, taken after Ar sputtering to measure bulk properties. The deconvolution procedure is described in the Experimental section.

ALD Deposition Temperature	Anneal Temperature	ALD Oxidant	M-O [%]	M-OH [%]	V_O [%]
150ºC	As-deposited	Thermal (H_2O)	89.4	6.9	3.7
150ºC	500ºC	Thermal (H_2O)	91.4	3.7	4.9
200ºC	As-deposited	Thermal (H_2O)	92.1	2.5	5.4
200ºC	500ºC	Thermal (H_2O)	92.9	3.5	4.6
200ºC	As-deposited	Hybrid	91.9	3.3	4.8
200ºC	500ºC	Hybrid	92.9	3.0	4.1

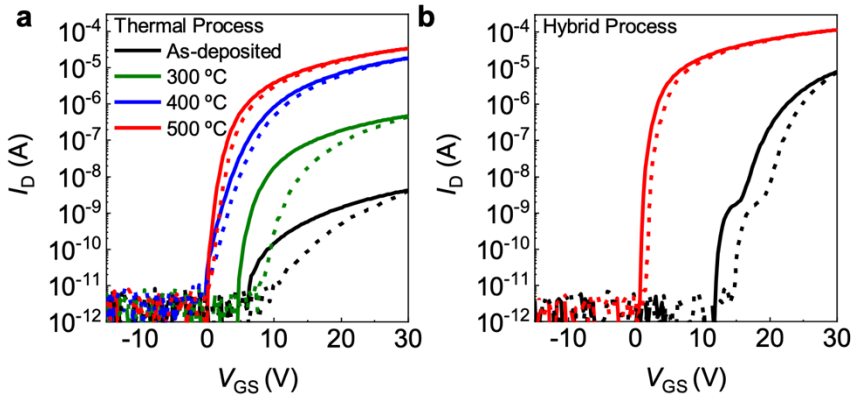

Figure S6. Transfer curves of ALD ZTO TFTs with f_{Sn} = 45% deposited at 150 ºC as a function of post-deposition anneal temperature for a) ZTO deposited using the thermal ALD process; and b) ZTO deposited using the hybrid ALD process. All TFTs have W/L of 10 and V_{DS} = 1 V. The forward *I-V* curves are indicated by the solid lines, and are identical to those shown in Figure 4a and Figure 4b. The reverse *I-V* curve sweeps are indicated by the dashed lines. The hysteresis, ΔV_C, between the forward and reverse sweeps is caused either by traps in the bulk of the film or by reactions at the back interface of the film.[3] Table 1 tabulates the hysteresis values.

Table S4. ZTO density for films with f_{Sn} = 45% determined by fitting the XRR spectra shown in Figure 2c and Figure S5a,b,c. The fitting method is described in the note below. For all films measured, the ZTO density increases with increased deposition temperature and more significantly following post-deposition anneals. For comparison, note that the density of SnO_2 is 6.85 g cm^{-3} and the density of ZnO is 5.6 g cm^{-3},[4] and a previous study on ALD ZTO using H_2O_2 as the oxidant reported ZTO density of 5.3 g cm^{-3}.[1]

ALD Deposition Temperature	ALD Process	Anneal Temperature	ZTO Density [g cm^{-3}]	% Change after Annealing
150 ºC	Thermal	As-deposited	5.0	
150 ºC	Thermal	300 ºC	5.4	8.0 %
150 ºC	Thermal	400 ºC	5.6	12.0 %
150 ºC	Thermal	500 ºC	5.7	14.0 %
200 ºC	Thermal	As-deposited	5.1	
200 ºC	Thermal	500 ºC	5.9	15.7 %
200 ºC	Hybrid	As-deposited	6.3	
200 ºC	Hybrid	500 ºC	6.5	3.2 %
200 ºC	Plasma	As-deposited	6.0	
200 ºC	Plasma	500 ºC	6.1	1.7 %

Note: To obtain ZTO density by XRR, we deposited ZTO on top of 100-nm thermally-grown SiO_2. We measured the thickness of SiO_2 by ellipsometry before ZTO deposition and measured the ZTO thickness after ZTO deposition and again after annealing. The thin film structure was then entered in the GlobalFit XRR software. The density of Si and SiO_2 were held fixed at the default values in the GlobalFit library. The initial density of the ZTO film was calculated based on the XPS atomic composition measurements. The experimental XRR data was then fit to determine the ZTO thickness and density.

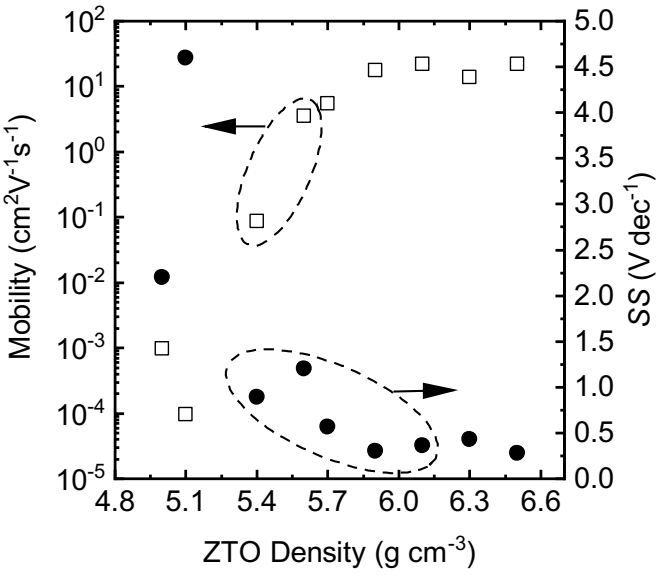

Figure S7. ALD ZTO TFT mobility (open squares) and sub-threshold slope (closed circles) plotted against ZTO density as measured by XRR. The numerical data can be found in Table 1, Table S2, and Table S4. The mobility correlates positively with film density, $r(7)=.894$, $p=.00116$, while the sub-threshold slope correlates negatively with density, $r(7)=.745$, $p=.021$, across all three ALD processes, deposition temperature, and post-deposition anneal temperature.

Table S5. Electrical properties of TFTs made using SiO_2 or Al_2O_3 gate insulator. The ZTO layer is deposited by thermal ALD at 150 ºC and annealed at 500 ºC. All ZTO films have 21% tin composition and were deposited during the same ALD run. The *I-V* behavior of these devices is shown in Figure 7a, and field-effect mobility as a function of gate-source voltage is shown in Figure 7c. The peak mobility is the maximum value obtained for the V_{GS} range shown.

Gate Insulator	Peak μ_{FE} [$cm^2V^{-1}s^{-1}$]a)	*SS* [V dec^{-1}]	ΔV_C [V]	V_{ON} [V]	V_{switch} [V]
SiO_2	5.44	0.57	0.89	0.54	6.84
Al_2O_3	5.39	0.23	0.55	0.70	2.06

Table S6. Electrical properties of TFTs made with different ZTO layer thicknesses. The ZTO layers are deposited by thermal ALD at 200 ºC and annealed at 500 ºC. All ZTO films have 21% tin composition. The *I-V* behavior of these devices is shown in Figure 7b, and field-effect mobility as a function of gate-source voltage is shown in Figure 7d. The last column gives the refractive index of the ZTO films measured by ellipsometry.

ZTO Thickness [nm]	μ_{FE} [$cm^2V^{-1}s^{-1}$]	*SS* [V dec^{-1}]	ΔV_C [V]	V_{On} [V]	Refractive Index
5	11.3	0.35	1.63	3.54	1.90
9	17.5	0.30	1.06	1.75	1.86
13	18.5	0.37	1.58	3.60	1.85

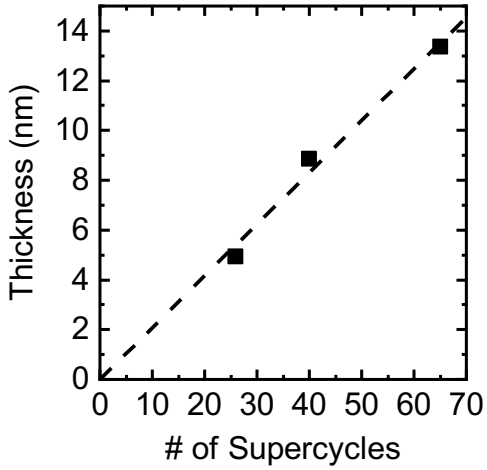

Figure S8. The number of supercycles vs. film thickness for the devices in Figure 7b and Table S6 are plotted with the black squares. The linear fit of the points going through the origin (black dashed line) indicates the films have a similar GPC and there is minimal nucleation delay for the 200 ºC thermal process.

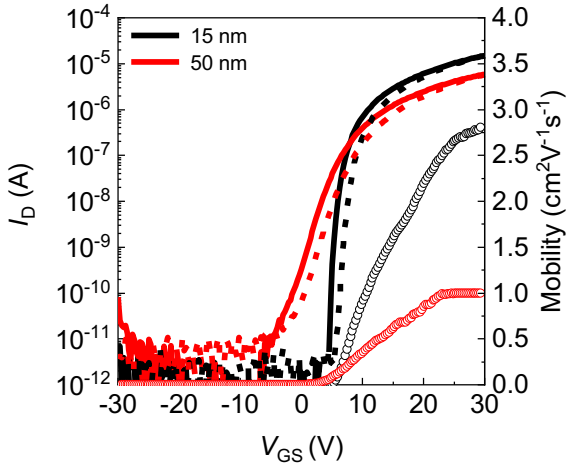

Figure S9. Transfer curves of TFTs with two different channel layer thickness. In both cases, the ZTO was deposited by thermal ALD at 130 ºC with f_{Sn} = 50%, and annealed at 500 °C. For both devices, W/L is 10 and V_{DS} = 1 V. The forward *I-V* curves are indicated by the solid lines while reverse curves are indicated by the dashed lines, all plotted on the left y-axis. Mobility is plotted using the open circles on the right y-axis. As ZTO film thickness increased from 15 nm to 50 nm, the mobility decreased from 2.7 $cm^2V^{-1}s^{-1}$ to ~1 $cm^2V^{-1}s^{-1}$. In addition, the *SS* increases substantially from 0.48 V dec^{-1} for the 15-nm thin film to ~ 1 V dec^{-1} for the 50-nm thick film. These results indicate that, at least for some ALD ZTO conditions, the channel layer thickness needs to be optimized in order to achieve the best TFT behavior.

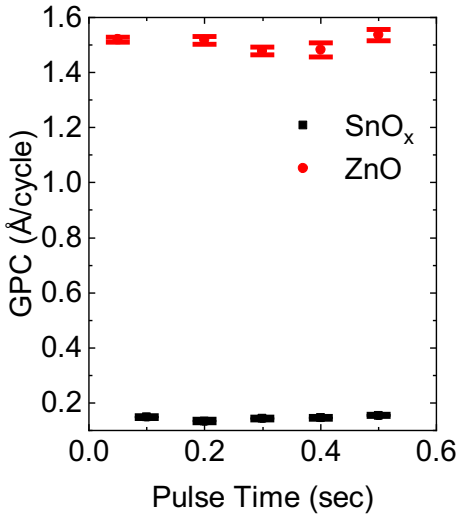

Figure S10. Binary saturation curves of ZnO (red) and SnO_x (black) at an ALD deposition temperature of 200 ºC. Film thickness was measured by ellipsometry. Error bars indicate uniformity across multiple samples placed in the deposition chamber during the same ALD run. For the pulse times tested, there is no significant change in growth-per-cycle (GPC), indicating that the films deposited at 200 ºC are within the ALD regime. We note that when the deposition temperature of the thermal ALD process is increased from 150ºC to 200ºC, the GPC of binary SnO_x is significantly reduced while the GPC of binary ZnO only decreases slightly. This leads to a thinner ZTO film achieved at 200 ºC for the same number of ALD cycles. As the deposition temperature increased, the tin composition stayed constant at 21%, perhaps due to increased suppression of ZnO growth within the ternary oxide under these deposition conditions.

Table S7. Growth conditions used for ZnO and SnO_x steps within the thermal ALD process. The binary GPC were measured by ellipsometry for films deposited at 200 °C.

Element	Precursor	Source Temp.	Pulse Time [sec]	Purge Time [sec]	Binary GPC [Å $cycle^{-1}$]
Zn	Diethylzinc (DEZ)	20 ºC	0.05	30	1.59
Sn	tetrakis(dimethylamino)tin (TDMASn)	65 ºC	0.2	30	0.15

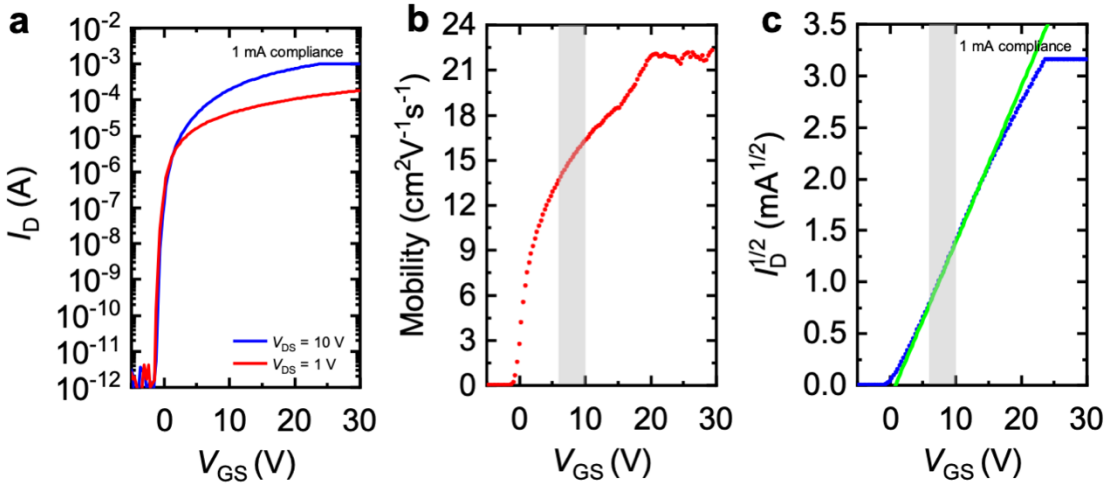

Figure S11. a) Transfer curves of 200 ºC hybrid ALD ZTO TFTs made with 21% tin composition films annealed at 500 ºC. b) Effective linear mobility versus V_{GS} extracted from the V_{DS} = 1 V curve in a). c) The square root of the drain current (blue circles) from the V_{DS} = 10 V curve in a). Saturation mobility is extracted using the equation $\mu_{sat} = \left(d\sqrt{I_D}/dV_{GS}\right)^2 2L(WC_{ox})^{-1}$ where *W, L, μ,* and C_{ox} refer to the channel width, channel length, electron mobility, and oxide capacitance, respectively. This fit, which is illustrated by the green line in Figure 11c, is performed for 6 V < V_{GS} < 10 V, the region indicated by the gray shaded area. This voltage range is chosen to ensure operation in the saturation regime, i.e. $V_{DS} > V_{GS} - V_t$, where V_t is ~0 V for this device. For this transistor, μ_{sat} = 13.2 $cm^2V^{-1}s^{-1}$, while the linear mobility extracted in the same V_{GS} region, shown in the gray shaded region in b), ranges from 13.7 $cm^2V^{-1}s^{-1}$ to 16.2 $cm^2V^{-1}s^{-1}$, with an average value of 15.0. Thus, for the same V_{GS} range, the saturation mobility and linear mobility agree within 13.6%. This indicates that the saturation mobility for a given V_{GS}-V_T is similar to the linear mobility in the same V_{GS}-V_T region. The blue lines in a,b) flattening out at 1 mA is due to the compliance current set during the measurement.

References

[1] J. Heo, S. Bok Kim, R. G. Gordon, *Applied Physics Letters* **2012**, *101*, 113507.

[2] B. D. Ahn, D. Choi, C. Choi, J.-S. Park, *Appl. Phys. Lett.* **2014**, *105*, 092103.
[3] M. Fakhri, H. Johann, P. Görrn, T. Riedl, *ACS Appl. Mater. Interfaces* **2012**, *4*, 4453.
[4] W. M. Haynes, Ed. , in *CRC Handbook of Chemistry and Physics, 97th Edition (Internet Version 2017)*, CRC Press/Taylor & Francis, Boca Raton, FL, **2017**.